ACS Synthetic Biology

pubs.acs.org/synthbio

Research Article

Sense-and-Respond Payload Delivery Using a Novel Antigen-Inducible Promoter Improves Suboptimal CAR-T Activation

Tingxi Guo,[⊥] Dacheng Ma,[⊥] and Timothy K. Lu*

Cite This: *ACS Synth. Biol.* 2022, 11, 1440−1453

Read Online

ACCESS | Metrics & More | Article Recommendations | Supporting Information

ABSTRACT: Chimeric antigen receptor (CAR)-T cell therapies demonstrate the clinical potential of lymphocytes engineered with synthetic properties. However, CAR-T cells are ineffective in most solid tumors, partly due to inadequate activation of the infused lymphocytes at the site of malignancy. To selectively enhance antitumor efficacy without exacerbating off-target toxicities, CAR-T cells can be engineered to preferentially deliver immunostimulatory payloads in tumors. Here, we report a novel antigen-inducible promoter for conditional payload expression in primary human T cells. In therapeutic T cell models, the novel NR4A-based promoter induced higher reporter gene expression than the conventional NFAT-based promoter under weakly immunogenic conditions, where payload expression is most needed. Minimal activity was detected from the inducible promoters in the absence of antigen and after withdrawal of stimulation. As a functional proof-of-concept, we used the NR4A-based promoter to express cytokines in an antimesothelin CAR-T model with suboptimal stimulation and observed improved proliferation compared to T cells engineered with the conventional NFAT promoter or CAR alone. Our system achieves CAR-directed payload expression under weakly immunogenic conditions and could enable the next generation of cell therapies with enhanced antitumor efficacy.

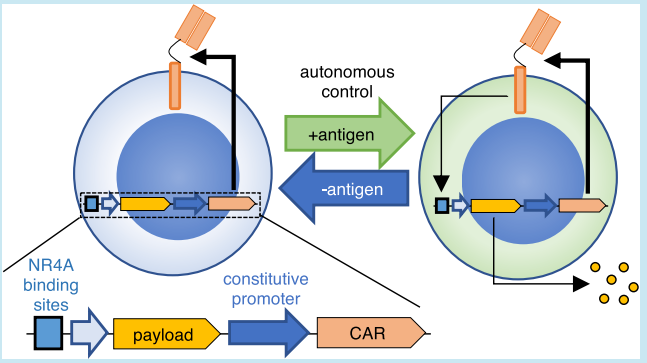

KEYWORDS: *inducible promoters, NR4A, NFAT, cell therapy, chimeric antigen receptors, engineered T cells*

INTRODUCTION

Genetically, programming cell functions with synthetic components holds promise for a variety of clinical applications.[1,2] A notable example is the adoptive transfer of T lymphocytes engineered with a chimeric antigen receptor (CAR) to treat cancer.[3−5] However, the consistent clinical benefit of these therapies has been largely limited to hematological malignancies. Most carcinomas remain non-responsive to CAR-T cells because the suppressive tumor microenvironment and variable antigen density prevent adequate activation of lymphocytes.[6−8] Amplifying the suboptimal responses of therapeutic T cells without exacerbating immune-mediated toxicity is a major unmet need for the treatment of solid tumors.

Beyond antigen receptors, adoptively transferred antitumor T cells can also be engineered to produce immunostimulatory payloads.[9] This strategy to augment immune responses can enhance the therapeutic properties of the infused T cells and reinvigorate endogenous immune cells. In preclinical models, T cells engineered to secrete common γ chain cytokines IL-2, IL-7, IL-15, and IL-21;[10] inflammatory cytokines IL-12,[11] IL-18,[12] and IL-23;[13] or other protein-based therapeutics[14,15] have demonstrated superior tumor control compared to nonproducers. The continuous secretion of stimulatory payloads, however, may counteract their beneficial effects. In one case, human T cells engineered to constitutively produce IL-15 resulted in the transformation of transductants in an IL-15 receptor-dependent manner.[16] Constitutive production of potent cytokines such as IL-2 or IL-18 also caused toxicities in preclinical CAR-T models.[10,12] These observations highlight the need to tightly control recombinant payload production and, ideally, restrict it to the tumor site to maximize its clinical benefit and prevent unwanted side effects.[17]

Synthetic promoters are capable of controlling and tuning transgene expression in response to a cellular pathway of interest.[18−20] A sensitive, antigen-inducible promoter with low background activity could leverage the preferential tumor reactivity of therapeutic receptors for localized payload delivery. The conventional approach for antigen-dependent transgene expression has been to use an NFAT-based promoter[21] encoding an NFAT/AP1 response element derived

Received: May 24, 2021
Published: March 22, 2022

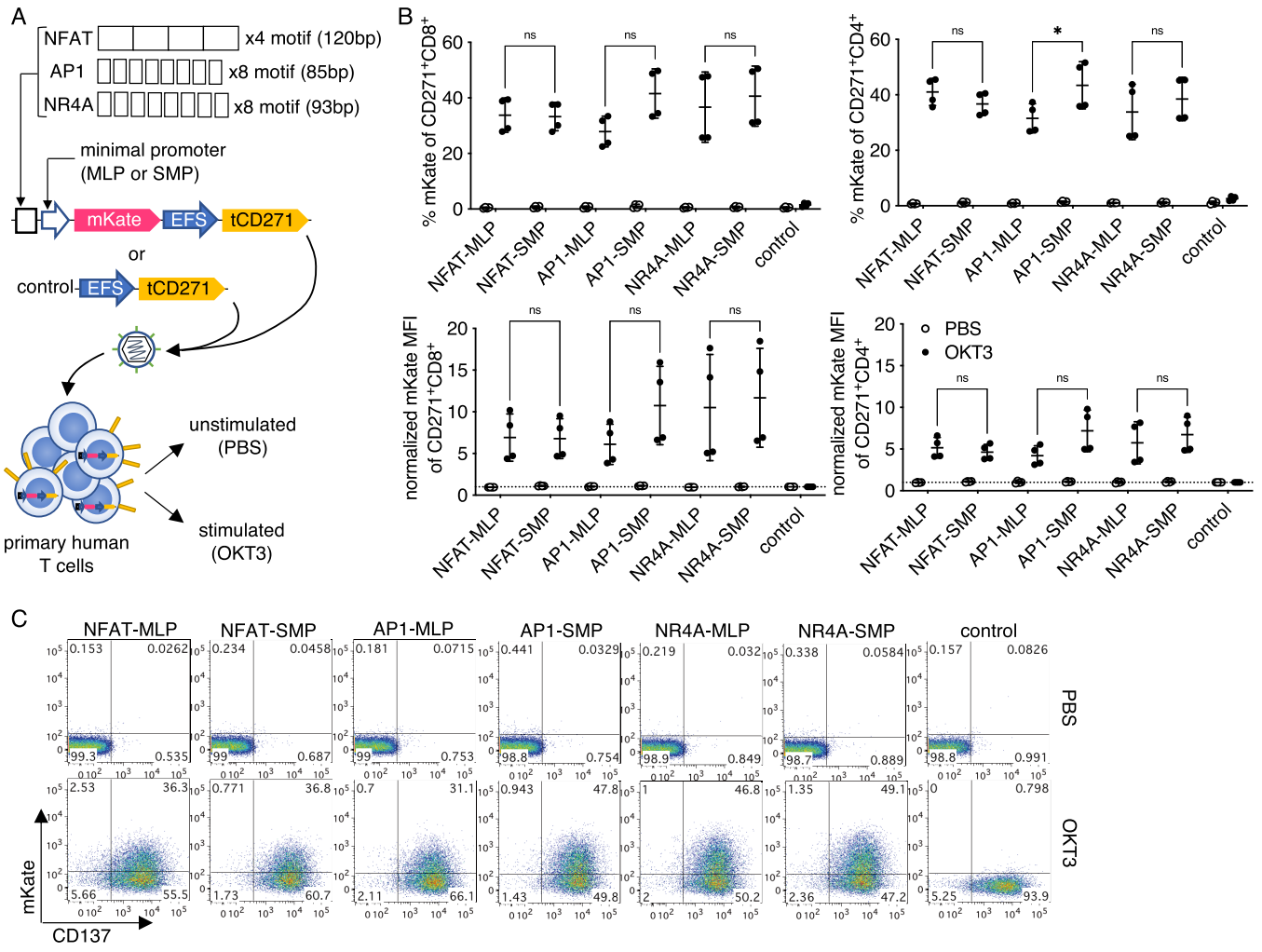

Figure 1. NFAT, API, and NR4A-based promoters are activated by anti-CD3 stimulation with minimal background. (a) Vector and experimental schematics. Response elements encoding NFAT, API, and NR4A-binding sites were cloned with either a core promoter from the adenovirus-derived major late promoter (MLP) or a synthetic minimal promoter (SMP). The NR4A and API binding motifs were spaced by three random nucleotides as described for the original SPECS library design. Lentiviral vectors were transduced to primary human T cells and treated with PBS or anti-CD3 clone OKT3. (b) Reporter fluorescence among transduced (CD271+) CD8+ or CD4+ cells were measured after 24 h. (c) Representative flow plots gated on CD271+ CD8+ T cells are shown. Lines and error bars denote mean ± standard deviation. ns—not significant, $*P < 0.05$ by two-way ANOVA adjusted for all possible comparisons using Tukey's test. $n = 4$ from two independent donors tested in two technical replicates.

from the human IL-2 enhancer.[22] This NFAT promoter was tested in the clinic to drive inducible expression of IL-12 and was transduced to *ex vivo* expanded tumor-infiltrating lymphocytes.[23] Toxicities were still observed after infusion, possibly because of the nonlocalized production of IL-12 by T cells with unknown antigen specificities. Subsequent preclinical developments have focused on combining the antigen-inducible NFAT promoter with a recombinant receptor[17,24] to better control the input signal for conditional payload expression. Despite its broad use, the standard NFAT promoter may not be the optimal choice for payload delivery.

Here, we identified a novel synthetic promoter based on an NR4A-binding motif that induced greater responses than the conventional NFAT promoter under weakly stimulatory conditions, which is when immune-enhancing molecules are most needed. Incorporating this synthetic promoter with a CAR in a lentiviral vector achieved automated payload response via sensing of the cognate tumor antigen. The engineered T cells respond to targets in an antigen-dependent manner and conditionally express a transgene of choice upon antigen engagement. The inducible promoter and vector design described here could enable future generations of synthetic lymphocytes, with controllable input and output to safely enhance therapeutic responses.

RESULTS AND DISCUSSION

Novel Antigen-Inducible Promoter Encoding an NR4A-Binding Motif. We previously generated a synthetic promoter library termed Synthetic Promoters with Enhanced Cell-State Specificity (SPECS), based on transcription factor (TF) binding motifs found in public databases. SPECS vectors were constructed by encoding repeated TF binding sites upstream of a minimal promoter derived from the adenoviral major late promoter (MLP) and mKate as the fluorescent reporter.[25] In the present study, to identify novel antigen receptor-inducible promoters from this library, we selected individual candidate promoters encoding binding sites for known TFs directly downstream of T cell receptor (TCR) signaling pathways (i.e., NFkB and MAPK targets),[22,26−32] or TFs upregulated upon TCR-induced activation.[33−40] TF

https://doi.org/10.1021/acssynbio.1c00236
ACS Synth. Biol. 2022, 11, 1440−1453

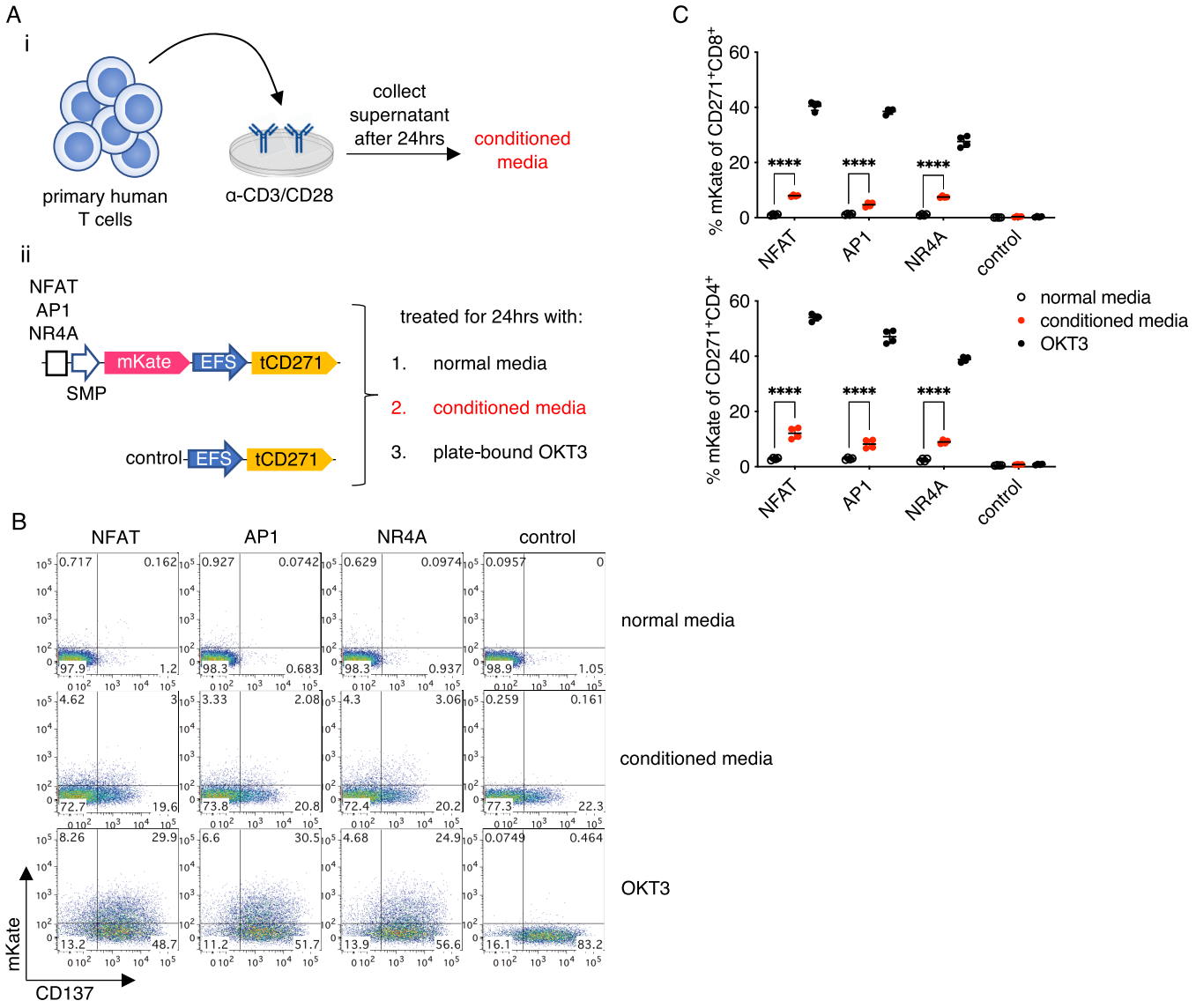

Figure 2. TCR-inducible promoters are weakly activated by an inflammatory milieu. (a) Experimental design. (i) Conditioned media was generated by collecting the supernatant from expanded primary human T cells restimulated with plate-bound anti-CD3/CD28 monoclonal antibodies. (ii) Promoter or control-transduced T cells were cultured with normal media, conditioned media, or plate-bound OKT3. (b) Representative flow plots gated on CD271+ CD8+ cells are shown. (c) Quantification of data shown in panel (b). Lines and error bars denote mean ± standard deviation. ****$P < 0.0001$ by two-way ANOVA adjusted for all possible comparisons using Tukey's test. $n = 4$ from two independent donors tested in two technical replicates.

binding site sequences ranged from 77 to 126 base pairs (bp) (Table S1). Twenty promoter vectors were individually transduced into primary human T cells by lentivirus and stimulated with plate-bound CD3 agonist OKT3, or left untreated as a control (Figure S1a). CD4 and CD8 T cell subsets responded similarly to OKT3 (Figure S1b). Among the tested promoters, the one encoding an NR4A-binding motif induced a high percentage of reporter positive cells (Figure S1b,d) and was selected for characterization. An AP1-based promoter was also chosen for comparison, given that it also induced a high response and that the AP1 pathway is well established in T cell activation.[41] As an internal positive control, antigen-mediated CD137 upregulation[42] was measured in all assays to ensure similar activation among experiments (Figure S1c).

Next, we compared SPECS-derived NR4A and AP1 promoters with the conventional NFAT promoter for OKT3-inducible responses. To facilitate quantitative comparisons, we introduced a second downstream transcription module into the lentiviral vector. In this module, the constitutive EFS promoter drives the expression of truncated CD271 (tCD271) to mark transduced cells. The EFS promoter was chosen for its compact size (~200 bp) and low enhancer-like activity.[43] We also tested an additional synthetic minimal promoter (SMP)[44] in combination with each of the three response elements (Figure 1a). The SMP and a similar variant enabled robust inducible promoter activity in human cells.[19,24] All of the promoter vectors transduced cells with comparable efficiency at ~60−80% (Figure S2a). As a negative control vector, we cloned the EFS-tCD271 module alone, without inducible promoters or mKate. All of the tested promoters responded similarly to the CD3 agonist among CD4 and CD8 subsets of primary human T cells after 1 day of stimulation (Figure 1b). In certain donors or in a TF-

https://doi.org/10.1021/acssynbio.1c00236
ACS Synth. Biol. 2022, 11, 1440−1453

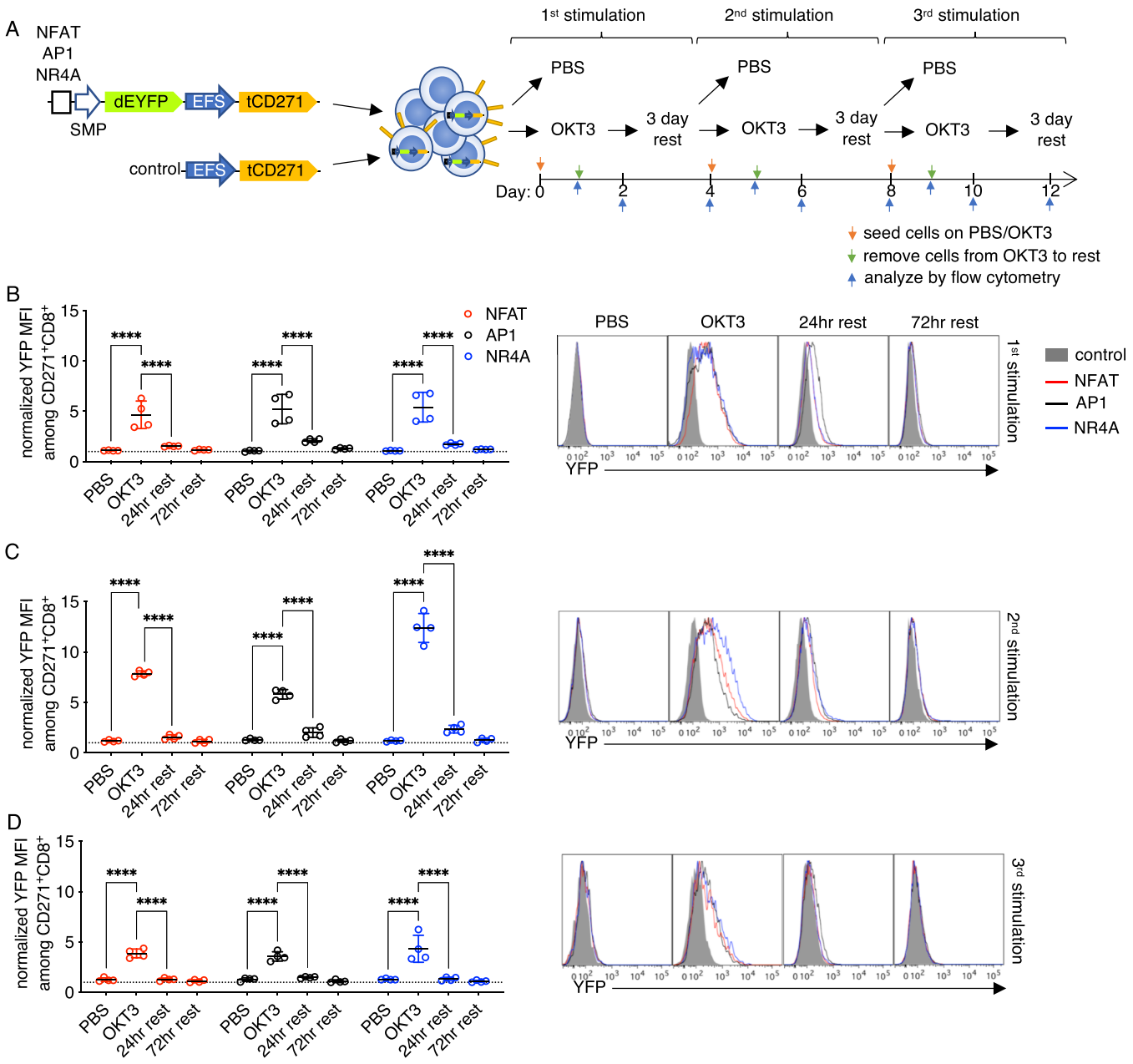

Figure 3. Inducible promoter responses are reversible and repeatable. (a) Vector and experimental schematics. Response elements encoding NFAT, API, and NR4A-binding sites with the synthetic minimal promoter (SMP) were used to drive destabilized yellow fluorescence protein (dEYFP). Lentiviral vectors were transduced to primary human T cells and treated with PBS or anti-CD3 clone OKT3 for 24 h and then transferred to a fresh plate for rest up to 3 days before repeating the process two more times. (b–d) Reporter fluorescence among CD271+ CD8+ cells were measured after 24 h of stimulation, then after 24 and 72 h of rest, following the first (b), second (c), and third (d) round. Fluorescence intensity was normalized to that of control vector transductants (see Figure S4a). Representative histograms gated on CD271+ CD8+ T cells are shown. Lines and error bars denote mean ± standard deviation. ****$P < 0.0001$ by two-way ANOVA adjusted for all possible comparisons using Tukey's test. $n = 4$ from two independent donors tested in two technical replicates.

dependent context, SMP performed better than MLP, although the two minimal promoters performed similarly well in most cases (Figure 1b,c). Thus, subsequent experiments were performed with SMP as the minimal promoter. No significant baseline activity in the absence of stimulation was observed with any of the inducible promoters (Figure 1b). Using a set of vectors with only a minimal promoter sequence upstream of mKate, we did not detect enhancer-like activity from the constitutive EFS promoter at the steady state or after activation, regardless of the choice of a minimal promoter (Figure S3).

To investigate whether TCR-inducible promoters could be activated by non-CD3-dependent mechanisms, we cultured promoter-transduced cells in conditioned media derived from strongly activated T cells to mimic an inflammatory milieu (Figure 2a). The NFAT, AP1, and NR4A promoters were significantly activated, albeit at similarly low levels (~10%) when the transduced cells were cultured in the conditioned media compared to normal media (Figure 2b,c). Reporter activity induced by the conditioned media was substantially lower than CD3-induced responses. Thus, we have identified a novel NR4A-based promoter with anti-CD3 inducible activity

https://doi.org/10.1021/acssynbio.1c00236
ACS Synth. Biol. 2022, 11, 1440–1453

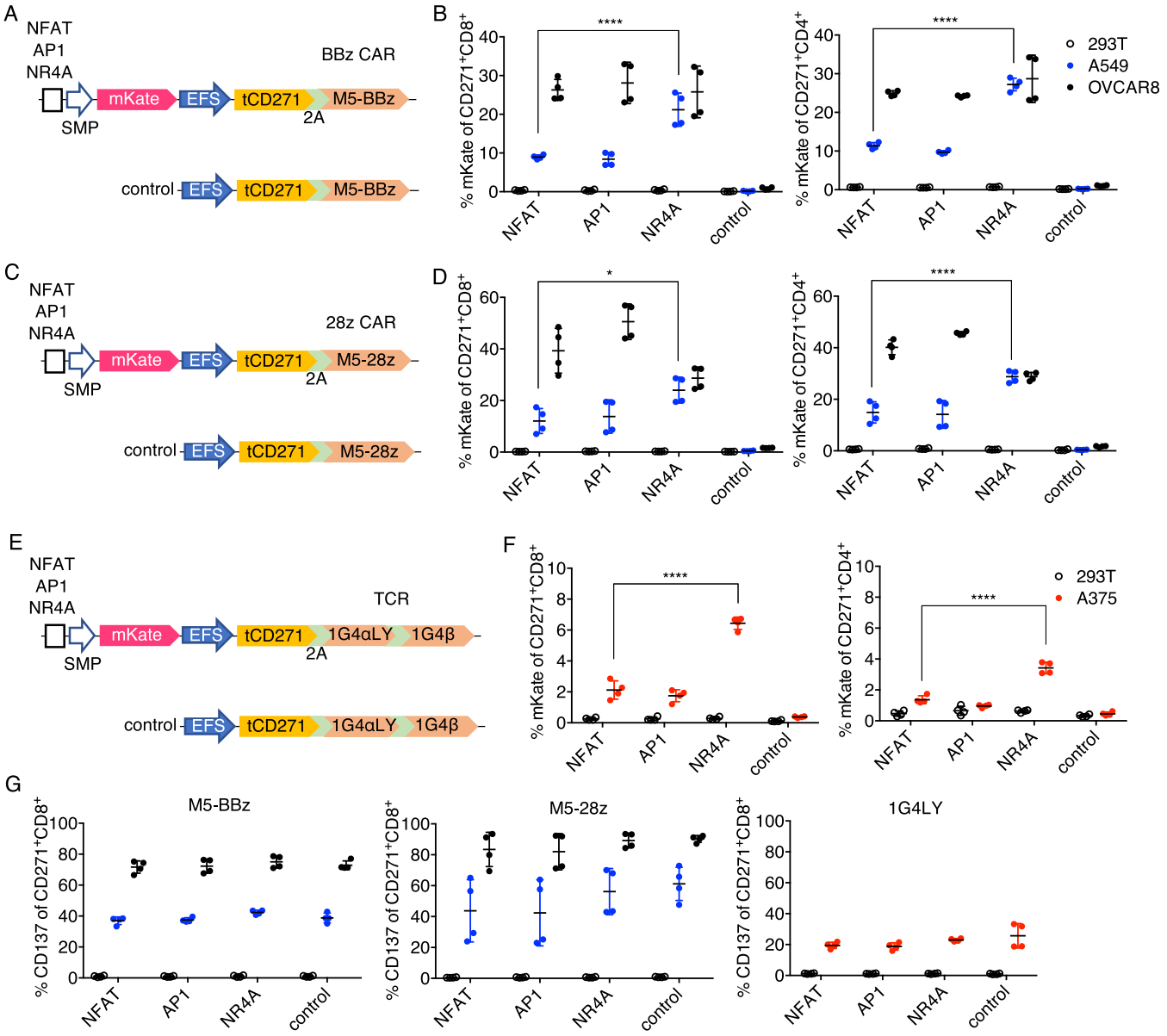

Figure 4. NR4A-based promoter responds better than NFAT or API in weakly stimulatory TCR/CAR-T models. (a, c, e) Schematics for CAR or TCR and inducible module encoded within a single vector. (b, d, f) Primary human T cells transduced with the vectors shown on the left of the respective graph were cocultured with the indicated target cells, and mKate fluorescence was measured after 24 h on CD271+ CD8+ or CD4+ subsets. (g) CD137 expression on CD271+ CD8+ T cells from the same experiments shown in panels (b, d, f). Lines and error bars denote mean ± standard deviation. *$P < 0.05$ and ****$P < 0.0001$ by two-way ANOVA adjusted for all possible comparisons using Tukey's test. $n = 4$ from two independent donors tested in two technical replicates.

and a single lentiviral vector system that permits stringent conditional gene expression alongside constitutive gene expression.

Inducible Promoters Demonstrate Reversible and Repeatable Activation. We next investigated the activity of the inducible promoters after the withdrawal of antigen receptor stimulation. Using the vectors shown in Figure 1a, we observed that it took up to 5 days after removing the source of stimulation for the mKate fluorescence to dissipate (Figure S2b), suggesting high stability of the fluorescent protein. To measure the reversibility and repeatability of inducible promoter activation, we changed the reporter to a destabilized enhanced yellow fluorescent protein (dEYFP) encoding an additional PEST motif, which reduces the half-life of fluorescent proteins.[45] In this system, the reporter fluorescence is more closely coupled to promoter activity. After transducing dEYFP vectors in human T cells, we stimulated the cells for 1 day with OKT3 as above and then transferred the cells to a fresh well without the agonist for 3 days of rest. This process was repeated three times (Figure 3a). The EFS-tCD271 vector served as a negative control for normalization, where the YFP mean fluorescence intensity (MFI) of cells transduced with each synthetic promoter vector was divided by that of the negative control vector (Figure S4a). Across three sequential stimulations, the NFAT, AP1, and NR4A promoter activities consistently returned to baseline after 3 days of rest in CD8 T cells. In fact, the fluorescence intensity for all reporters was reduced by at least 50% after only 1 day (Figure 3b–d).

Interestingly, normalized responses were moderately higher after the second stimulation (Figures 3b,c and S5a), akin to a

https://doi.org/10.1021/acssynbio.1c00236
ACS Synth. Biol. 2022, 11, 1440−1453

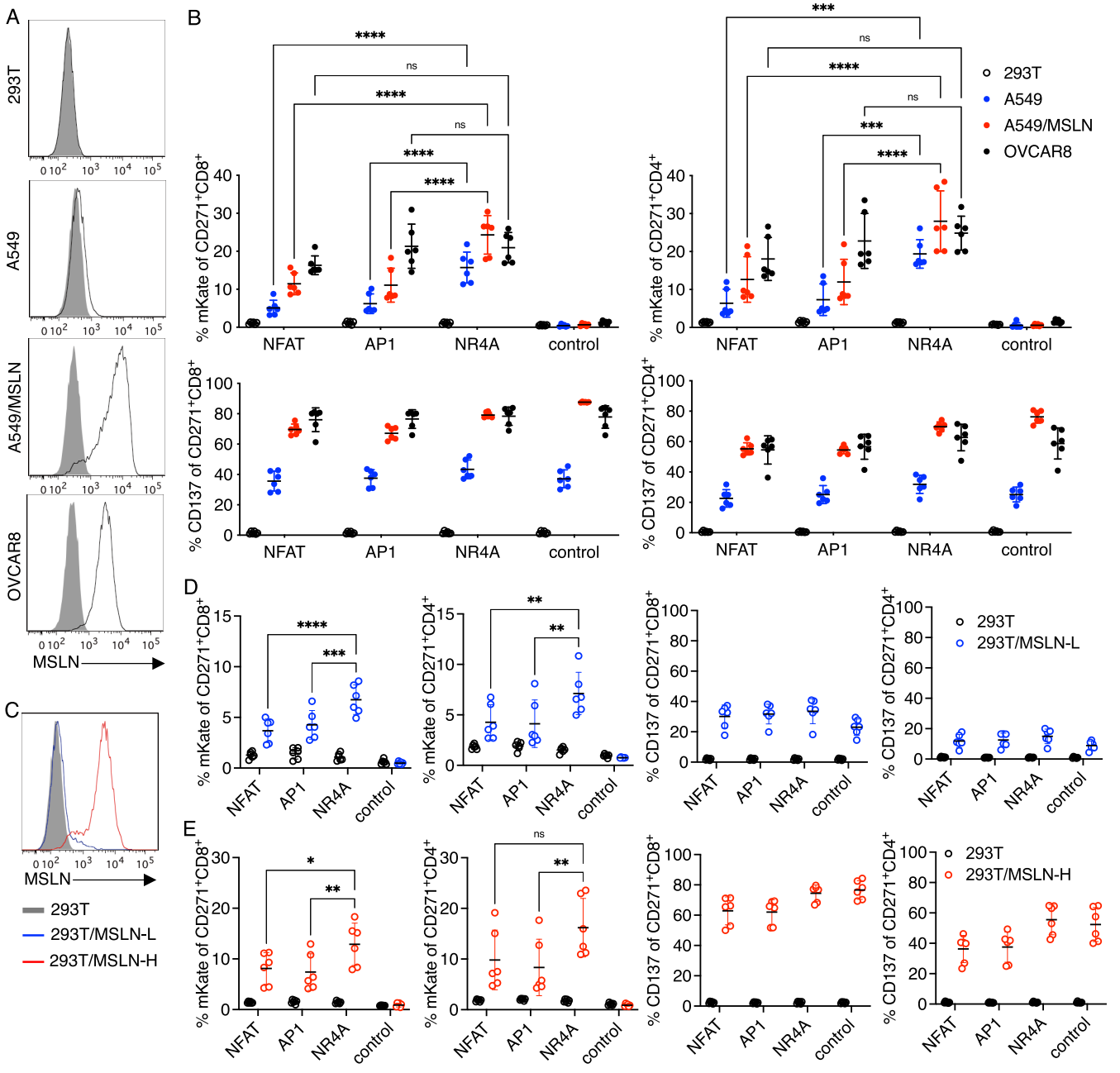

Figure 5. NR4A-based promoter induces higher or comparable responses to NFAT in a target cell-dependent manner. (a) Surface mesothelin (MSLN) expression on the indicated target cells lines. A549 was transduced via lentivirus with full-length human MSLN expressed under the EFS promoter to generate A549/MSLN. Gray solid and black lines indicate control and antigen-specific staining, respectively. (b) Primary human T cells transduced with the vectors shown in Figure 4a were cocultured with the targets in a percent of mKate (top) and CD137 (bottom) expression was measured after 24 h on CD271+ CD8+ or CD4+ subsets. (c) MSLN staining of 293T and 293T expressing low (L) or high (H) levels of MSLN. 293T was transduced with MSLN by lentivirus and sorted by flow cytometry to generate low- and high-antigen target cells. (d, e) CAR-T cells as described in (b) were cocultured with the indicated 293T target cells. CD137 and mKate expression on CD271+ CD8+ or CD4+ subsets were measured after 24 h after coculture with 293T/MSLN-L (d) or 293T/MSLN-H (e) targets. Lines and error bars denote mean ± standard deviation. ns—not significant, $*P < 0.05$, $**P < 0.01$, $***P < 0.001$, and $****P < 0.0001$ by two-way ANOVA adjusted for all possible comparisons using Tukey's test. $n = 6$ from two independent donors tested in three technical replicates.

recall response in adaptive lymphocytes. The lower responses observed after the third stimulation (Figures 3d and S5a) were likely the result of activation-induced cell death (Figure S4c). Reversible responses were also observed in CD4 T cells with at least one round of stimulation (Figure S5b). Repeated OKT3 stimulation biased the outgrowth of CD4− cells and decreased the overall viability of most samples (Figure S5c); thus, the promoter responses in the CD4 subset after multiple rounds of activation could not be reliably measured. Throughout the course of the experiment, the proportion of CD271+ cells did not change significantly (Figure S5d), indicating that repeated activation of the promoters was well tolerated and did not cause a growth disadvantage.

NR4A Promoter Induces Higher Responses than NFAT and AP1 in Weakly Immunogenic, Therapeutically Relevant Models. Although OKT3 is a potent activator

https://doi.org/10.1021/acssynbio.1c00236
ACS Synth. Biol. 2022, 11, 1440−1453

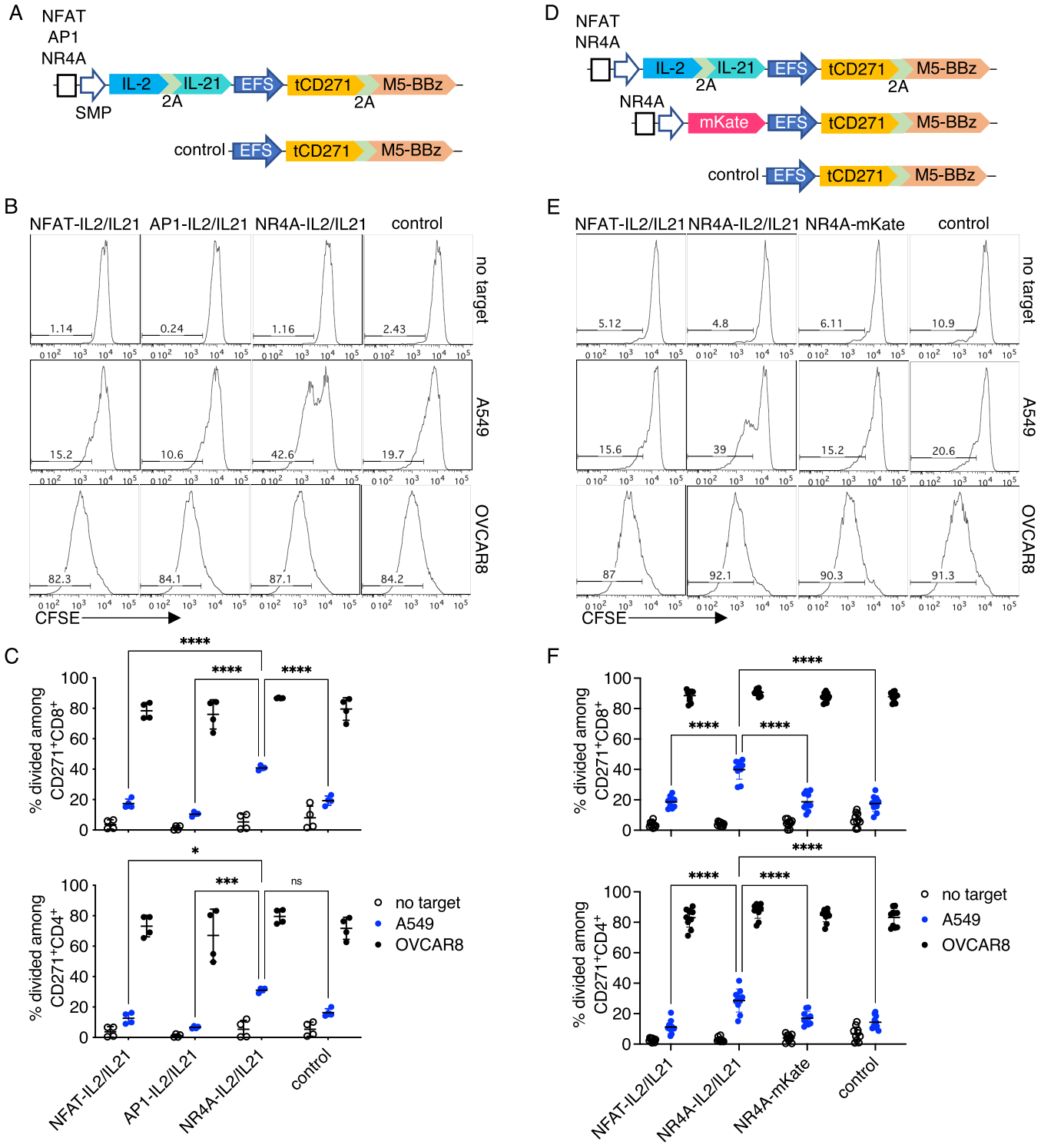

Figure 6. Cytokines delivered under the NR4A-based promoter amplify weak proliferative responses in CAR-T cells. (a) Schematics for vectors encoding M5-BBz CAR with or without IL-2 and IL-21 as inducible payloads. (b) Primary human T cells transduced with the vectors shown in (a) were labeled with CFSE and cocultured with the indicated target cells. Dye dilution was measured after 4 days of coculture. Representative histograms gated on CD271+ CD8+ T cells are shown. (c) Quantification of CFSE dilution among CD271+ CD8+ or CD4+ subsets. $n = 4$ from two independent donors tested in two technical replicates. (d) Schematics for vectors encoding IL-2 and IL-21 as inducible payloads or mKate as a control. (e) Experiment was performed as described in (b). Representative histograms gated on CD271+ CD8+ T cells are shown. (f) Quantification of CFSE dilution among CD271+ CD8+ or CD4+ subsets. $n = 10$ from three independent donors, with two donors tested in four technical replicates and one donor tested in two technical implicates. Lines and error bars denote mean ± standard deviation, ns—not significant, $^{*}P < 0.05$, $^{***}P < 0.001$, and $^{****}P < 0.0001$ by two-way ANOVA adjusted for all possible comparisons using Tukey's test.

of T cells, it is not representative of therapeutically relevant receptor−antigen interactions. To characterize inducible promoter responses in more appropriate models, we first selected a CAR based on the humanized single-chain variable

https://doi.org/10.1021/acssynbio.1c00236
ACS Synth. Biol. 2022, 11, 1440−1453

fragment (scFv) M5, targeting the widely expressed mesothelin tumor antigen.[46] The M5 CAR, which encodes 41BB and CD3z signaling domains (M5-BBz), is currently being tested in clinical trials for treating a variety of solid tumors (NCT03054298, NCT03323944). Mesothelin-targeting CAR-T strategies have yet to yield consistent objective responses[47] and, therefore, could benefit from the addition of inducible payloads. To investigate the inducible promoter activity in a CAR setting, the M5-BBz CAR and tCD271, separated by a porcine 2A (P2A) sequence, were encoded downstream of the EFS promoter for constitutive expression. In these constructs, inducible promoters that drive the expression of mKate as a reporter were cloned upstream of the CAR. tCD271 with the receptor alone served as a control vector (Figure 4a). T cells were transduced with the vectors and stimulated with HEK293T (no mesothelin), A549 (low mesothelin), or OVCAR8 (high mesothelin) target cells[48,49] (Figure 5a).

Among the transduced CD8 and CD4 T cells, we observed no mKate fluorescence when effector cells were cultured with HEK293T, again demonstrating minimal antigen-independent promoter activity (Figure 4b). With the strong OVCAR8 stimulation, similar levels of reporter expression were observed. Notably, the NR4A promoter induced significantly more mKate expression than the NFAT and AP1 promoters when cultured with weakly stimulatory A549 targets (Figures 4b, S6a, and S7a). OVCAR8 cells were indeed more immunogenic than A549 cells in the M5 model based on CD137 upregulation (Figures 4g and S6a). A similar trend was observed when the promoters were tested with a CD28-based M5 CAR (M5-28z, Figure 4c): the NR4A promoter responded at higher levels than the standard NFAT in response to A549 stimulation (Figures 4d and S6a). In the M5-28z model, AP1 demonstrated higher activity than NR4A in response to OVCAR8 cells (Figures 4d and S7b). Inducible promoter vectors for both CARs were transduced at ∼50−70% efficiency (Figure S6b), with comparable CD271 expression levels between the NR4A and NFAT promoter vectors (Figure S6c).

Next, we constructed a similar set of vectors using the affinity-matured HLA-A2/NYESO1-specific 1G4 TCR[50] as the model antigen receptor. 1G4 TCR has demonstrated clinical efficacy in treating melanoma and synovial sarcoma.[51,52] The two P2A sequences between tCD271, TCRα, and TCRβ genes were codon-modified to avoid repetition in the viral genome (Figure 4e). TCR-T cells were stimulated with HEK293T or A375 cells. Both of these cell lines express HLA-A2, but only A375 expresses the cognate antigen.[50,53] In the TCR model, NR4A also responded with consistently higher reporter positivity than NFAT or AP1 after coculture with A375, although the overall responses were lower than those seen with the CAR models. The promoters induced higher responses in CD8 T cells than in CD4 cells (Figures 4f and S7c), which was expected since the 1G4 TCR is HLA class I restricted. The lower levels of CD137 upregulation in the TCR model were consistent with the weaker promoter activity (Figure 4g), which may have been caused by the insufficient formation of the correct TCRα/β pairing. A stronger constitutive promoter may be needed to practically implement this system with recombinant TCRs, which must be expressed at high levels to compete with endogenous TCR hemichains in forming antigen-specific surface receptors. The TCR constructs were ∼400 bp larger than the CAR vectors and were transduced less efficiently (Figure S6b). Nevertheless, across all of the receptor models tested in our study, we observed significantly higher responses with the NR4A-based promoter compared to the responses observed with the standard NFAT promoter under poorly stimulatory conditions—precisely the context where payload expression is needed.

Characterizing Mesothelin-Induced Promoter Responses in M5-BBz CAR-T Cells. To evaluate the antigen-induced promoter responses in more detail, we further characterized the antigen-inducible promoters using the M5-BBz CAR with additional target cells expressing various levels of mesothelin. First, we overexpressed mesothelin on A549 cells to generate A549/MSLN cells with high levels of surface antigen (Figure 5a). When M5-BBz CAR-T cells encoding the NFAT, AP1, or NR4A-mKate reporter constructs (Figure 4a) were stimulated with A549, OVCAR8, or A549/MSLN cells, or with 293T cells as a control, the NR4A-based promoter induced higher and comparable reporter expression in response to A549 and OVCAR8, respectively, versus the NFAT and AP1 promoters, as observed in Figure 4b. When stimulated with A549/MSLN targets with high-antigen expression, the NR4A promoter also induced higher responses than other promoters (Figures 5b and S8), suggesting that the NR4A promoter may be more active than NFAT in some highly stimulatory contexts as well. A549/MSLN stimulation indeed activated more CAR-T responders than A549 based on CD137 upregulation (Figure 5b).

We then generated 293T cells expressing low (L) or high (H) levels of mesothelin to investigate the effect of antigen density on an independent target cell line. Parental 293T cells without mesothelin expression were transduced with the antigen and sorted by flow cytometry to generate 293T/MSLN-L and 293T/MSLN-H targets that resemble A549 and A549/MSLN, respectively (Figure 5c). The NR4A-based promoter induced significantly higher reporter expression when CAR-T cells were stimulated with 293T/MSLN-L cells compared to NFAT and AP1 promoters (Figures 5d and S8), although the differences were less pronounced than those seen with A549-induced responses (Figure 5b). Stimulation with 293T/MSLN-H cells also elicited significantly higher responses from the NR4A promoter in CD8+ CAR-T cells (Figure 5e). Collectively, these data demonstrate that the NR4A-based promoter consistently outperforms the conventional NFAT promoter not only under weakly stimulatory conditions but also in certain high-antigen settings in a target cell-dependent manner, where target cell-specific factors may contribute to differential activation of the promoters.

Recombinant Cytokines Expressed under the NR4A Promoter Amplify Weak Antitumor Proliferative Responses. As a proof-of-concept, we generated inducible constructs to conditionally express IL-2 and IL-21 in the clinically relevant M5-BBz model. The mKate reporter gene of M5-BBz CAR vectors (Figure 4a) was replaced with recombinant IL-2 and IL-21, separated by a P2A sequence (Figure 6a). Constitutive expression of either cytokine alone has been reported to enhance the proliferation of CD19 CAR-T cells.[10] Although both of these common γ chain cytokines can be produced endogenously by activated human T cells, cytokine production is poor when the cells are suboptimally stimulated.[54] Therefore, we reasoned that the NR4A-based synthetic promoter system could supplement these beneficial cytokines under conditions that preclude endogenous production.

https://doi.org/10.1021/acssynbio.1c00236
ACS Synth. Biol. 2022, 11, 1440−1453

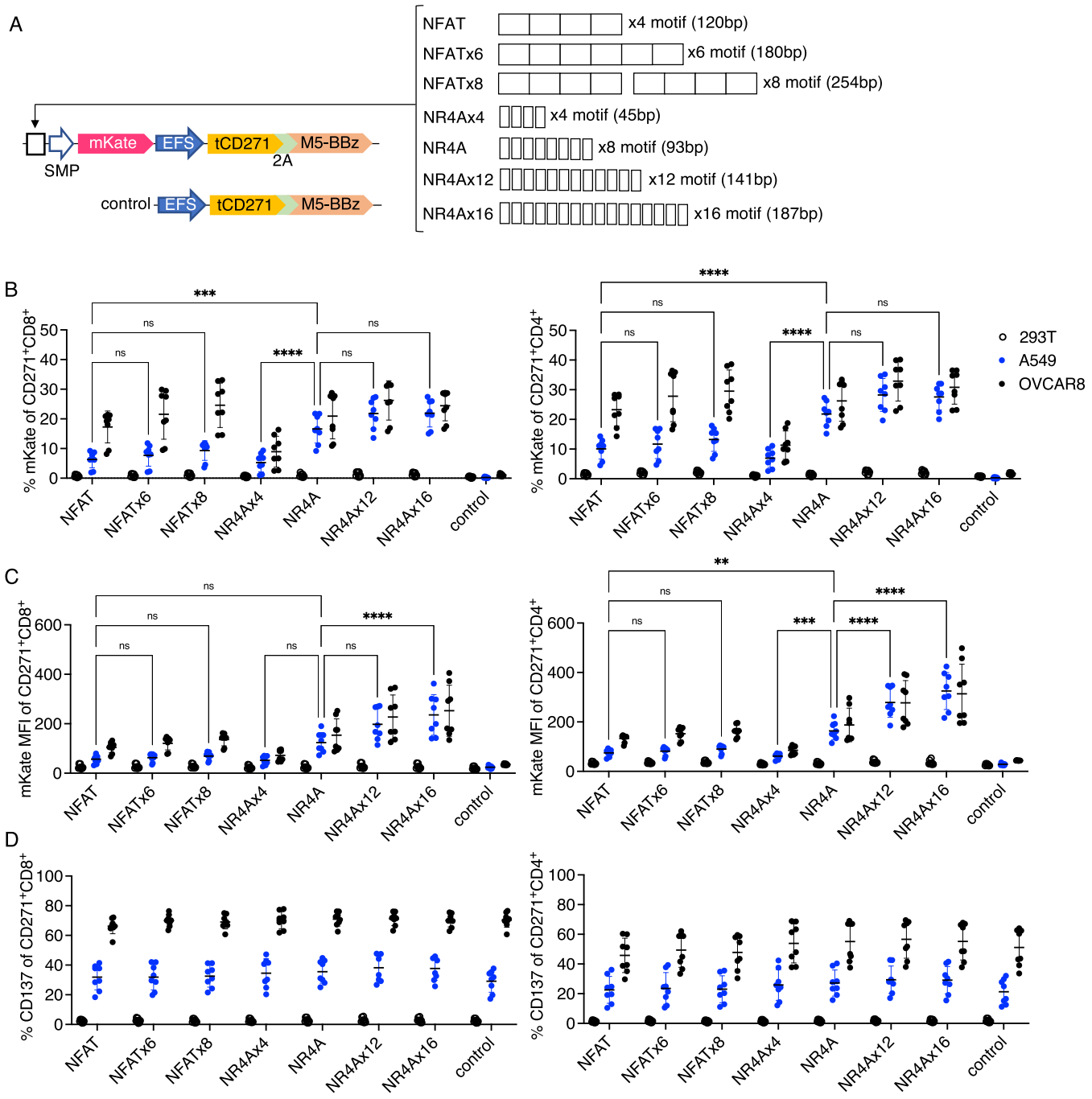

Figure 7. Increasing transcription factor binding sites modestly improves the activity of the NR4A-based but not NFAT-based promoter. (a) Schematics for M5-BBz CAR vectors encoding various copies of NFAT or NR4A-binding sites. Attempts to clone eight direct copies of the NFAT motif were unsuccessful. Thus, NFATx8 was generated with a 14 bp spacer between two parental NFAT response elements of four motifs each (120 + 120 + 14 = 254 bp). Full sequences are shown in Supporting Information Tables. Primary human T cells transduced with the vectors shown in (a) were cocultured with the indicated target cells. Percent of mKate positivity (b), mKate MFI (c), and percent of CD137 positivity (d) on CD271+ CD8+ or CD4+ subsets were quantified. n = 8 from two independent donors tested in four technical replicates. Lines and error bars denote mean ± standard deviation. ns—not significant, $^{**}P < 0.01$, $^{***}P < 0.001$, and $^{****}P < 0.0001$ by two-way ANOVA adjusted for all possible comparisons using Tukey's test.

In a proliferation assay without cytokine supplementation in the media, CAR-T cells transduced with the control M5-BBz or inducible IL-2/IL-21 vectors demonstrated low levels of proliferation in the absence of stimulation. In contrast, the majority of the cells were divided after coculture with the immunogenic OVCAR8 cells with high-antigen expression. When stimulated with weakly immunogenic A549 targets, more of the NR4A-IL-2/IL-21 transductants proliferated compared to cells engineered with other vectors. The improvement in proliferation was more pronounced for the CD8 than CD4 subset (Figure 6b,c), consistent with a past study showing that IL-2 improves the proliferation of suboptimally stimulated CD8 but not of CD4 murine T cells.[55] Based on additional experiments in which the NR4A

https://doi.org/10.1021/acssynbio.1c00236
ACS Synth. Biol. 2022, 11, 1440−1453

promoter induced the expression either of cytokines or mKate as a control (Figure 6d), we determined that the enhanced proliferation in response to A549 was payload-dependent (Figure 6e,f). Transduction efficiencies of inducible cytokine constructs were similar (Figures S9 and S10c).

Consistent with these data, more of the CAR-T cells encoding the NR4A-IL-2/IL-21 module produced IL-2 when stimulated with A549, compared to cells transduced with other inducible modules or the control vector (Figure S10a,b). Moreover, in A549 cocultures, the proliferation of NFAT-IL-2/IL-21 CAR-T cells was not increased compared to control CAR-T cells (Figure 6c,f), in line with the low responses observed with the NFAT promoter in Figure 4b. Across these experiments, inducible expression of the cytokines did not significantly enhance proliferation compared to CAR alone when cells were cultured with OVCAR8 cells (Figure 6c,f). In summary, these data demonstrate a proof-of-concept that payloads delivered via the NR4A promoter system can augment suboptimal CAR-T responses.

Increasing the Number of TF Binding Sites Modestly Improves Activity of NR4A Based but Not NFAT-Based Promoter. Finally, we investigated the effect of TF binding site multiplicity on the responsiveness of the novel NR4A promoter and the conventional NFAT promoter, using the inducible mKate reporter within the M5-BBz mesothelin CAR-T model. We generated additional NFAT-based promoters with six and eight motif copies and NR4A-based promoters with 4, 12, and 16 motif copies. Due to the compactness of the NR4A motif, more binding sites could be tested compared to NFAT; the NR4Ax16 response element was comparable in length to the NFATx6 (Figure 7a and Table S2).

Increasing the number of NFAT binding motifs from four to eight copies did not augment promoter responses when CAR-T cells were cocultured with A549 cells (Figure 7b,c). For NR4A-based promoters, whereas additional binding sites did not increase the proportion of cells responding after stimulation (Figure 7b), the mean intensity of reporter fluorescence was modestly higher with 16 versus 8 copies of the NR4A-binding motif when transductants were stimulated with the low antigen A549 targets (Figure 7c). Conversely, reducing NR4A-binding sites from eight to four copies significantly diminished responses when CAR-T cells were stimulated with either A549 or OVCAR8 targets (Figure 7b). Encoding promoters with varying numbers of NFAT or NR4A-binding sites had no effect on CAR-T activation as measured by CD137 upregulation (Figure 7c). These data indicate that the NFAT promoter activity in our system cannot be improved by increasing the number of TF binding sites, and the parental NFAT and NR4A promoters encoding four and eight binding sites, respectively, are likely sufficient for near-maximal responses.

CONCLUSIONS

In this study, we identified a novel antigen-inducible transcriptional response element in human T cells based on a TF binding site of the NR4A family. Notably, the NR4A-based promoter outperformed the conventional NFAT-based promoter under poorly stimulatory conditions. TCR-induced activation of the NR4A pathway has been characterized previously.[37,56,57] This pathway has been used to monitor TCR signaling by knocking-in a reporter at the NR4A1 (Nur77) locus.[57−59] In theory, payload transgenes could also be knocked-in at the NR4A1 site to achieve inducible expression, and improvements in site-specific integration technologies for primary lymphocytes[60−62] will facilitate the practical implementation of this approach. With the knock-in method, however, transcriptional output will be dictated by endogenous elements, which lacks the flexibility afforded by a synthetic promoter system that can be tuned for a variety of applications.

Our promoter platform similarly leverages the NR4A pathway; instead of relying on endogenous response elements to drive NR4A1 transcription, a short sequence encoding an NR4A-binding motif is used to drive conditional gene expression. The NR4A family consists of three members: NR4A1/Nur77, NR4A2/Nurr1, and NR4A3/Nor1, all of which bind to the same consensus DNA motif.[63] Thus, all three members are likely to be involved in regulating our synthetic promoter. In human T cells, NR4A1 expression is dependent on phosphoinositide 3-kinase and mitogen-activated protein kinase (MAPK) pathways of antigen receptor signaling but is largely independent of NFAT.[56] In murine T cells, NR4A1 is similarly regulated as in humans, whereas NR4A2 and NR4A3 require both NFAT and MAPK pathways for full induction.[64]

Efforts to develop alternatives to NFAT-based antigen-inducible promoters have also been reported by other groups. Recently, Webster et al.[65] described an antigen-inducible promoter encoding both AP1 and NFKB motifs with low basal activity. Placing a CAR and other payloads under the AP1-NFKB promoter led to the self-amplifying expression of the transgenes in an antigen-dependent manner.[65] Wei and Jensen assembled a library of promoters composed of binding sites targeted by TFs upregulated in antigen-activated T cells (WO2018/213332). Screening the library in T cells identified promoters with greater inducible activity than the conventional NFAT in a CD19 CAR-T model. Notably, neither study tested the NR4A motif described here. Whether the sensitivity of these antigen-inducible promoters can be improved by incorporating the NR4A motif warrants investigation.

Activation at a lower immunogenic threshold is a critical feature of the NR4A antigen-inducible promoter that could widen the therapeutic index for a variety of molecular therapeutics compared to systemic or constitutive delivery. Our findings could also guide the design of subsequent antigen-inducible promoters with even greater sensitivity and robustness, to enable applications such as site-specific production of: bispecific engagers to trigger bystander lymphocyte responses; chemokines to promote infiltration of immune effectors; or cell-intrinsic regulators to conditionally reprogram engineered cells in an autonomous manner. These and other applications can be explored in future preclinical studies. In conclusion, the outcomes of this study could potentially empower a wide range of synthetic biology approaches to overcome current challenges in adoptive cell immunotherapies.

MATERIAL AND METHODS

Cell Culture. HEK293T, A375, A549, and Jurkat.E6 cell lines were obtained from the American Type Culture Collection (ATCC, Manassas, VA). OVCAR8 was a gift from Dr. Sangeeta N. Bhatia (Massachusetts Institute of Technology, Cambridge, MA). HEK293T, A375, A549, and OVCAR8 cell lines were cultured in DMEM (Thermo Fisher Scientific, Waltham, MA; catalog #10569010). Primary human T cells and the Jurkat.E6 cell line were cultured in RPMI-1640 (Thermo Fisher Scientific; catalog #11875119). All media

https://doi.org/10.1021/acssynbio.1c00236
ACS Synth. Biol. 2022, 11, 1440−1453

were supplemented with 10% fetal bovine serum (Corning; catalog #35-010-CV) and 1% penicillin/streptomycin (Thermo Fisher Scientific; catalog #15140122).

Generation of Lentiviral Vectors. Truncated CD271 (tCD271)-CAR or TCR, EYFP destabilized with a PEST motif (dEYFP), full-length human mesothelin (MSLN, UniProt: Q13421-1), and IL-2/IL-21 fragments were synthesized as gBlocks by Integrated DNA Technologies (Coralville, IA). The M5 scFv sequence was derived from the patent WO2015/090230. Sequences of 28z and BBz signaling domains and the affinity-matured 1G4 TCR were as previously described.[50,66] Except NFAT, all TF binding sites and mKate sequences were derived from SPECS plasmids (Addgene #127842). The NFAT response element, containing four binding motifs, was subcloned from the pSIRV-NFAT-eGFP plasmid[67] (a gift from Peter Steinberger, Addgene plasmid #118031). Two copies of the NFAT sequence were combined with an intervening restriction site to generate the NFATx8 response element. NFATx6, NR4Ax4, NR4Ax12, and NR4Ax16 were synthesized as oligos by IDT. The EYFP sequence was derived from Addgene plasmid #51791, and the PEST sequence was derived from Addgene plasmid #69072. The EFS promoter was subcloned from the lentiCRISPRv2 plasmid (a gift from Feng Zhang, Addgene plasmid #52961). The EFS promoter and tCD271-CAR/TCR fragments were first assembled into a lentiviral backbone vector (derived from pFUGW in-house) in the reverse orientation of the long-terminal repeats. Inducible promoter and reporter or payload genes were then inserted upstream of the EFS promoter. Inserted sequences were confirmed by Sanger sequencing (GENEWIZ, South Plainfield, NJ). Vector component sequences can be found in Table S2. Each set of NFAT, AP1, or NR4A vectors only differed at the TF binding sequence.

Lentivirus Production. Lentivirus was generated by transfecting HEK293T cells of less than 10 passages and grown to ∼80% confluency in T25 flasks, with 1.5 μg of pMD2.G (a gift from Didier Trono, Addgene plasmid #12259), 3.5 μg of psPAX2 (a gift from Didier Trono, Addgene plasmid #12260), and 5 μg of respective transfer plasmid using the TransIT-2020 reagent (MirusBio, Japan). Media was changed to fresh complete DMEM 16−24 h post transfection, and lentivirus was collected after another 24 h to be used immediately or stored at −80 °C. The virus was titered by infecting Jurkat.E6 at limiting dilutions.

Lentiviral Transduction of Primary Human T Cells. Peripheral blood mononuclear cells (PBMCs) were isolated by density gradient centrifugation from apheresis products of healthy donors (Brigham and Women's Hospital Crimson Core, Boston, MA). Primary human T cells were purified from PBMCs by Pan T Cell Isolation Kit (Miltenyi Biotec, Germany). Purified T cells were stimulated with anti-CD3/CD28 Dynabeads (Thermo Fisher Scientific) at a T cell/bead ratio of 1:2. After 24 h, Dynabeads were removed and stimulated T cells were seeded on a Retronectin (Takara Bio, Japan)-coated nontissue culture-treated plate with virus and centrifuged at 1200*g*, 32 °C for 30 min. One-time infection was carried out for the smaller vectors shown in Figures 1 and 2 at a multiplicity of infection (MOI) of 5−10. Larger vectors shown in Figures 3 and 4 were infected at a MOI of 10−20, spread out over 2 days of daily infection. During stimulation and infection, T cells were supplemented daily with 100 U/mL of IL-2 and 10 ng/mL of IL-15 (NCI Preclinical Repository, Frederick, MD). After infection, T cells were maintained by supplementing with 100 U/mL of IL-2 and 10 ng/mL of IL-15 every 3 days. T cells were expanded for another 5−6 days after the last infection prior to use in experiments.

Flow Cytometry. The following monoclonal antibodies (BioLegend, San Diego, CA) were used in this study: antihuman CD3 (clone UCHT1), antihuman CD4 (clone RPA-T4), antihuman CD8 (clone RPA-T8), antihuman CD271 (clone ME20.4), antihuman mesothelin (clone MN), polyclonal goat antimouse IgG, antihuman CD69 (clone FN50), antihuman CD137 (clone 4B4-1), and antihuman IL-2 (clone MQ1-17H12). Surface staining of T cells was carried out at 4 °C for 15 min with a master mix of antibodies. Target cells were stained with antimesothelin mAb, then washed and stained with polyclonal antimouse IgG antibodies, or with antimouse IgG alone as a control staining. For intracellular staining of IL-2, cells were fixed and permeabilized after surface staining using the Cytofix/Cytoperm kit (BD Biosciences). Stained cells were analyzed with a FACSCantoII, FACSCelesta, or LSRFortessa flow cytometer (BD Biosciences). Data analysis was performed with FlowJo. All data shown were gated on singlets and live cells, determined by Aqua fixable dye (Thermo Fisher Scientific) for mKate-expressing and intracellular experiments or 7-aminoactinomycin D (BioLegend) for all other experiments.

T Cell Stimulation Assays. For plate-bound stimulations, nontissue culture-treated plates were coated with 2 μg/mL anti-CD3 clone OKT3 (NCI preclinical repository) with or without 2 μg/mL anti-CD28 clone CD28.2 (BioLegend) by incubating at 4 °C overnight. The same volume of PBS (Thermo Fisher Scientific) was used as a control treatment. Antibody or PBS solution was removed, and T cells were seeded to the treated wells and cultured for 24 h. Cells were analyzed post stimulation or transferred to fresh tissue-culture-treated wells to rest. For cell-based coculture stimulations, T cells were mixed with HEK293T, A375, A549, or OVCAR8 targets at an effector/target (ET) ratio of 3:1 and cultured for 24 h to measure reporter fluorescence. For intracellular IL-2 detection, CAR-T cells were cultured with targets at a 3:1 ET ratio for 18 h, followed by treatment with 1500× diluted monesin (BD Biosciences) for 6 h. To measure proliferation, T cells were washed with PBS and labeled with 1 μM of carboxyfluorescein succinimidyl ester (CFSE, Thermo Fisher Scientific) by incubating them at 37 °C for 5 min. Labeled cells were washed with complete media and cocultured with A549 or OVCAR8 target cells at an ET ratio of 10:1. CFSE dilution was assessed after 4 days of coculture.

Statistics. Comparisons between more than two groups were performed by two-way analysis of variance (ANOVA) with Tukey's multiple comparisons test. Differences were considered significant at an adjusted *P*-value of less than 0.05. All statistical analyses were performed using GraphPad Prism 9. Error bars denote one standard deviation.

■ ASSOCIATED CONTENT

Supporting Information

The Supporting Information is available free of charge at https://pubs.acs.org/doi/10.1021/acssynbio.1c00236.

Additional functional characterizations of antigen-inducible promoters and supporting data for main figures (Figures S1−S11); vector component sequences used in this study (Tables S1 and S2) (PDF)

https://doi.org/10.1021/acssynbio.1c00236
ACS Synth. Biol. 2022, 11, 1440−1453

AUTHOR INFORMATION

Corresponding Author

Timothy K. Lu − *Synthetic Biology Group, Research Laboratory of Electronics, Massachusetts Institute of Technology, Cambridge, Massachusetts 02139, United States; Synthetic Biology Center, Department of Biological Engineering and Department of Electrical Engineering and Computer Science, Massachusetts Institute of Technology, Cambridge, Massachusetts 02139, United States; Senti Biosciences, South San Francisco, California 94080, United States;* orcid.org/0000-0002-3918-8923; Phone: 617-715-4808; Email: timlu@mit.edu; Fax: 619-789-4808

Authors

Tingxi Guo − *Synthetic Biology Group, Research Laboratory of Electronics, Massachusetts Institute of Technology, Cambridge, Massachusetts 02139, United States*

Dacheng Ma − *Synthetic Biology Group, Research Laboratory of Electronics, Massachusetts Institute of Technology, Cambridge, Massachusetts 02139, United States*

Complete contact information is available at: https://pubs.acs.org/10.1021/acssynbio.1c00236

Author Contributions

⊥T.G. and D.M. contributed equally. T.G., D.M., and T.K.L. designed the experiments, analyzed the data, and wrote the manuscript. T.G. and D.M. performed the experiments. T.K.L. supervised the study.

Notes

The authors declare the following competing financial interest(s): T.K.L. is a co-founder of Senti Biosciences, Synlogic, Engine Biosciences, Tango Therapeutics, Corvium, BiomX, Eligo Biosciences, Bota.Bio, and Avendesora. T.K.L. also holds financial interests in nest.bio, Ampliphi, IndieBio, MedicusTek, Quark Biosciences, Personal Genomics, Thryve, Lexent Bio, MitoLab, Vulcan, Serotiny, and Avendesora. Other authors declare no competing interests.

ACKNOWLEDGMENTS

This work was supported in part by the Department of Defense (W81XWH-17-1-0159, W81XWH-16-1-0565) and National Institutes of Health (5-R33-AI121669-04). T.G. was supported by a Postdoctoral Fellowship from the Natural Sciences and Engineering Research Council of Canada. The authors thank the flow cytometry core facility at the Koch Institute for Integrative Cancer Research at Massachusetts Institute of Technology. The authors thank Karen Pepper for editing the manuscript.

ABBREVIATIONS

CAR, chimeric antigen receptor; IL, interleukin; TCR, T cell receptor

REFERENCES

(1) Teixeira, A. P.; Fussenegger, M. Engineering mammalian cells for disease diagnosis and treatment. *Curr. Opin. Biotechnol.* **2019**, *55*, 87−94.

(2) Dudek, R. M.; Chuang, Y.; Leonard, J. N. Engineered Cell-Based Therapies: A Vanguard of Design-Driven Medicine. In *A Systems Biology Approach to Blood*; Advances in Experimental Medicine and Biology; Springer, 2014; Vol. *844*, pp 369−391.

(3) Lim, W. A.; June, C. H. The Principles of Engineering Immune Cells to Treat Cancer. *Cell* **2017**, *168*, 724−740.

(4) Sadelain, M.; Riviere, I.; Riddell, S. Therapeutic T cell engineering. *Nature* **2017**, *545*, 423−431.

(5) Hong, M.; Clubb, J. D.; Chen, Y. Y. Engineering CAR-T Cells for Next-Generation Cancer Therapy. *Cancer Cell* **2020**, *38*, 473−488.

(6) Anderson, K. G.; Stromnes, I. M.; Greenberg, P. D. Obstacles Posed by the Tumor Microenvironment to T cell Activity: A Case for Synergistic Therapies. *Cancer Cell* **2017**, *31*, 311−325.

(7) Shah, N. N.; Fry, T. J. Mechanisms of resistance to CAR T cell therapy. *Nat. Rev. Clin. Oncol.* **2019**, *16*, 372−385.

(8) Hou, A. J.; Chen, L. C.; Chen, Y. Y. Navigating CAR-T cells through the solid-tumour microenvironment. *Nat. Rev. Drug Discovery* **2021**, *20*, 531−550.

(9) Yeku, O. O.; Brentjens, R. J. Armored CAR T-cells: utilizing cytokines and pro-inflammatory ligands to enhance CAR T-cell anti-tumour efficacy. *Biochem. Soc. Trans.* **2016**, *44*, 412−418.

(10) Markley, J. C.; Sadelain, M. IL-7 and IL-21 are superior to IL-2 and IL-15 in promoting human T cell-mediated rejection of systemic lymphoma in immunodeficient mice. *Blood* **2010**, *115*, 3508−3519.

(11) Koneru, M.; Purdon, T. J.; Spriggs, D.; Koneru, S.; Brentjens, R. J. IL-12 secreting tumor-targeted chimeric antigen receptor T cells eradicate ovarian tumors in vivo. *Oncoimmunology* **2015**, *4*, No. e994446.

(12) Hu, B.; Ren, J.; Luo, Y.; Keith, B.; Young, R. M.; Scholler, J.; Zhao, Y.; June, C. H. Augmentation of Antitumor Immunity by Human and Mouse CAR T Cells Secreting IL-18. *Cell Rep.* **2017**, *20*, 3025−3033.

(13) Ma, X.; Shou, P.; Smith, C.; Chen, Y.; Du, H.; Sun, C.; Porterfield Kren, N.; Michaud, D.; Ahn, S.; Vincent, B.; Savoldo, B.; Pylayeva-Gupta, Y.; Zhang, S.; Dotti, G.; Xu, Y. Interleukin-23 engineering improves CAR T cell function in solid tumors. *Nat. Biotechnol.* **2020**, *38*, 448−459.

(14) Choi, B. D.; Yu, X.; Castano, A. P.; Bouffard, A. A.; Schmidts, A.; Larson, R. C.; Bailey, S. R.; Boroughs, A. C.; Frigault, M. J.; Leick, M. B.; Scarfo, I.; Cetrulo, C. L.; Demehri, S.; Nahed, B. V.; Cahill, D. P.; Wakimoto, H.; Curry, W. T.; Carter, B. S.; Maus, M. V. CAR-T cells secreting BiTEs circumvent antigen escape without detectable toxicity. *Nat. Biotechnol.* **2019**, *37*, 1049−1058.

(15) Rafiq, S.; Yeku, O. O.; Jackson, H. J.; Purdon, T. J.; van Leeuwen, D. G.; Drakes, D. J.; Song, M.; Miele, M. M.; Li, Z.; Wang, P.; Yan, S.; Xiang, J.; Ma, X.; Seshan, V. E.; Hendrickson, R. C.; Liu, C.; Brentjens, R. J. Targeted delivery of a PD-1-blocking scFv by CAR-T cells enhances anti-tumor efficacy in vivo. *Nat. Biotechnol.* **2018**, *36*, 847−856.

(16) Hsu, C.; Jones, S. A.; Cohen, C. J.; Zheng, Z.; Kerstann, K.; Zhou, J.; Robbins, P. F.; Peng, P. D.; Shen, X.; Gomes, T. J.; Dunbar, C. E.; Munroe, D. J.; Stewart, C.; Cornetta, K.; Wangsa, D.; Ried, T.; Rosenberg, S. A.; Morgan, R. A. Cytokine-independent growth and clonal expansion of a primary human CD8+ T-cell clone following retroviral transduction with the IL-15 gene. *Blood* **2007**, *109*, 5168−5177.

(17) Chmielewski, M.; Abken, H. TRUCKs: the fourth generation of CARs. *Expert Opin. Biol. Ther.* **2015**, *15*, 1145−1154.

(18) Saxena, P.; Bojar, D.; Fussenegger, M. Design of Synthetic Promoters for Gene Circuits in Mammalian Cells. In *Mammalian Synthetic Promoters*; Methods in Molecular Biology; Humana, 2017; Vol. *1651*, pp 263−273.

(19) Ede, C.; Chen, X.; Lin, M. Y.; Chen, Y. Y. Quantitative Analyses of Core Promoters Enable Precise Engineering of Regulated Gene Expression in Mammalian Cells. *ACS Synth. Biol.* **2016**, *5*, 395−404.

(20) Nissim, L.; Wu, M. R.; Pery, E.; Binder-Nissim, A.; Suzuki, H. I.; Stupp, D.; Wehrspaun, C.; Tabach, Y.; Sharp, P. A.; Lu, T. K. Synthetic RNA-Based Immunomodulatory Gene Circuits for Cancer Immunotherapy. *Cell* **2017**, *171*, 1138−1150.e15.

(21) Zhang, L.; Kerkar, S. P.; Yu, Z.; Zheng, Z.; Yang, S.; Restifo, N. P.; Rosenberg, S. A.; Morgan, R. A. Improving adoptive T cell therapy by targeting and controlling IL-12 expression to the tumor environment. *Mol. Ther.* **2011**, *19*, 751−759.

(22) Fiering, S.; Northrop, J. P.; Nolan, G. P.; Mattila, P. S.; Crabtree, G. R.; Herzenberg, L. A. Single cell assay of a transcription

factor reveals a threshold in transcription activated by signals emanating from the T-cell antigen receptor. *Genes Dev.* **1990**, *4*, 1823−1834.
(23) Zhang, L.; Morgan, R. A.; Beane, J. D.; Zheng, Z.; Dudley, M. E.; Kassim, S. H.; Nahvi, A. V.; Ngo, L. T.; Sherry, R. M.; Phan, G. Q.; Hughes, M. S.; Kammula, U. S.; Feldman, S. A.; Toomey, M. A.; Kerkar, S. P.; Restifo, N. P.; Yang, J. C.; Rosenberg, S. A. Tumor-infiltrating lymphocytes genetically engineered with an inducible gene encoding interleukin-12 for the immunotherapy of metastatic melanoma. *Clin. Cancer Res.* **2015**, *21*, 2278−2288.
(24) Zimmermann, K.; Kuehle, J.; Dragon, A. C.; Galla, M.; Kloth, C.; Rudek, L. S.; Sandalcioglu, I. E.; Neyazi, B.; Moritz, T.; Meyer, J.; Rossig, C.; Altvater, B.; Eiz-Vesper, B.; Morgan, M. A.; Abken, H.; Schambach, A. Design and Characterization of an "All-in-One" Lentiviral Vector System Combining Constitutive Anti-G(D2) CAR Expression and Inducible Cytokines. *Cancers* **2020**, *12*, No. 375.
(25) Wu, M. R.; Nissim, L.; Stupp, D.; Pery, E.; Binder-Nissim, A.; Weisinger, K.; Enghuus, C.; Palacios, S. R.; Humphrey, M.; Zhang, Z.; Maria Novoa, E.; Kellis, M.; Weiss, R.; Rabkin, S. D.; Tabach, Y.; Lu, T. K. A high-throughput screening and computation platform for identifying synthetic promoters with enhanced cell-state specificity (SPECS). *Nat. Commun.* **2019**, *10*, No. 2880.
(26) Rincón, M.; Flavell, R. A. AP-1 transcriptional activity requires both T-cell receptor-mediated and co-stimulatory signals in primary T lymphocytes. *EMBO J.* **1994**, *13*, 4370−4381.
(27) Kim, H. P.; Leonard, W. J. CREB/ATF-dependent T cell receptor-induced FoxP3 gene expression: a role for DNA methylation. *J. Exp. Med.* **2007**, *204*, 1543−1551.
(28) Muthusamy, N.; Barton, K.; Leiden, J. M. Defective activation and survival of T cells lacking the Ets-1 transcription factor. *Nature* **1995**, *377*, 639−642.
(29) Youn, H. D.; Sun, L.; Prywes, R.; Liu, J. O. Apoptosis of T cells mediated by Ca2+-induced release of the transcription factor MEF2. *Science* **1999**, *286*, 790−793.
(30) Li, Y.; Sedwick, C. E.; Hu, J.; Altman, A. Role for protein kinase Ctheta (PKCtheta) in TCR/CD28-mediated signaling through the canonical but not the non-canonical pathway for NF-kappaB activation. *J. Biol. Chem.* **2005**, *280*, 1217−1223.
(31) Charvet, C.; Auberger, P.; Tartare-Deckert, S.; Bernard, A.; Deckert, M. Vav1 couples T cell receptor to serum response factor-dependent transcription via a MEK-dependent pathway. *J. Biol. Chem.* **2002**, *277*, 15376−15384.
(32) Malcolm, T.; Chen, J.; Chang, C.; Sadowski, I. Induction of chromosomally integrated HIV-1 LTR requires RBF-2 (USF/TFII-I) and Ras/MAPK signaling. *Virus Genes* **2007**, *35*, 215−223.
(33) Safford, M.; Collins, S.; Lutz, M. A.; Allen, A.; Huang, C. T.; Kowalski, J.; Blackford, A.; Horton, M. R.; Drake, C.; Schwartz, R. H.; Powell, J. D. Egr-2 and Egr-3 are negative regulators of T cell activation. *Nat. Immunol.* **2005**, *6*, 472−480.
(34) de la Roche, M.; Ritter, A. T.; Angus, K. L.; Dinsmore, C.; Earnshaw, C. H.; Reiter, J. F.; Griffiths, G. M. Hedgehog signaling controls T cell killing at the immunological synapse. *Science* **2013**, *342*, 1247−1250.
(35) Glasmacher, E.; Agrawal, S.; Chang, A. B.; Murphy, T. L.; Zeng, W.; Vander Lugt, B.; Khan, A. A.; Ciofani, M.; Spooner, C. J.; Rutz, S.; Hackney, J.; Nurieva, R.; Escalante, C. R.; Ouyang, W.; Littman, D. R.; Murphy, K. M.; Singh, H. A genomic regulatory element that directs assembly and function of immune-specific AP-1-IRF complexes. *Science* **2012**, *338*, 975−980.
(36) Ho, I. C.; Hodge, M. R.; Rooney, J. W.; Glimcher, L. H. The proto-oncogene c-maf is responsible for tissue-specific expression of interleukin-4. *Cell* **1996**, *85*, 973−983.
(37) Woronicz, J. D.; Calnan, B.; Ngo, V.; Winoto, A. Requirement for the orphan steroid receptor Nur77 in apoptosis of T-cell hybridomas. *Nature* **1994**, *367*, 277−281.
(38) Wu, Z.; Kim, H. P.; Xue, H. H.; Liu, H.; Zhao, K.; Leonard, W. J. Interleukin-21 receptor gene induction in human T cells is mediated by T-cell receptor-induced Sp1 activity. *Mol. Cell. Biol.* **2005**, *25*, 9741−9752.
(39) Chikuma, S.; Suita, N.; Okazaki, I. M.; Shibayama, S.; Honjo, T. TRIM28 prevents autoinflammatory T cell development in vivo. *Nat. Immunol.* **2012**, *13*, 596−603.
(40) von Essen, M. R.; Kongsbak, M.; Schjerling, P.; Olgaard, K.; Odum, N.; Geisler, C. Vitamin D controls T cell antigen receptor signaling and activation of human T cells. *Nat. Immunol.* **2010**, *11*, 344−349.
(41) Foletta, V. C.; Segal, D. H.; Cohen, D. R. Transcriptional regulation in the immune system: all roads lead to AP-1. *J. Leukocyte Biol.* **1998**, *63*, 139−152.
(42) Wolfl, M.; Kuball, J.; Ho, W. Y.; Nguyen, H.; Manley, T. J.; Bleakley, M.; Greenberg, P. D. Activation-induced expression of CD137 permits detection, isolation, and expansion of the full repertoire of CD8+ T cells responding to antigen without requiring knowledge of epitope specificities. *Blood* **2007**, *110*, 201−210.
(43) Zychlinski, D.; Schambach, A.; Modlich, U.; Maetzig, T.; Meyer, J.; Grassman, E.; Mishra, A.; Baum, C. Physiological promoters reduce the genotoxic risk of integrating gene vectors. *Mol. Ther.* **2008**, *16*, 718−725.
(44) Merlet, E.; Lipskaia, L.; Marchand, A.; Hadri, L.; Mougenot, N.; Atassi, F.; Liang, L.; Hatem, S. N.; Hajjar, R. J.; Lompré, A. M. A calcium-sensitive promoter construct for gene therapy. *Gene Ther.* **2013**, *20*, 248−254.
(45) Li, X.; Zhao, X.; Fang, Y.; Jiang, X.; Duong, T.; Fan, C.; Huang, C. C.; Kain, S. R. Generation of destabilized green fluorescent protein as a transcription reporter. *J. Biol. Chem.* **1998**, *273*, 34970−34975.
(46) Morello, A.; Sadelain, M.; Adusumilli, P. S. Mesothelin-Targeted CARs: Driving T Cells to Solid Tumors. *Cancer Discovery* **2016**, *6*, 133−146.
(47) Haas, A. R.; Tanyi, J. L.; O'Hara, M. H.; Gladney, W. L.; Lacey, S. F.; Torigian, D. A.; Soulen, M. C.; Tian, L.; McGarvey, M.; Nelson, A. M.; Farabaugh, C. S.; Moon, E.; Levine, B. L.; Melenhorst, J. J.; Plesa, G.; June, C. H.; Albelda, S. M.; Beatty, G. L. Phase I Study of Lentiviral-Transduced Chimeric Antigen Receptor-Modified T Cells Recognizing Mesothelin in Advanced Solid Cancers. *Mol. Ther.* **2019**, *27*, 1919−1929.
(48) Ho, M.; Bera, T. K.; Willingham, M. C.; Onda, M.; Hassan, R.; FitzGerald, D.; Pastan, I. Mesothelin expression in human lung cancer. *Clin. Cancer Res.* **2007**, *13*, 1571−1575.
(49) Tang, Z.; Feng, M.; Gao, W.; Phung, Y.; Chen, W.; Chaudhary, A.; St Croix, B.; Qian, M.; Dimitrov, D. S.; Ho, M. A human single-domain antibody elicits potent antitumor activity by targeting an epitope in mesothelin close to the cancer cell surface. *Mol. Cancer Ther.* **2013**, *12*, 416−426.
(50) Robbins, P. F.; Li, Y. F.; El-Gamil, M.; Zhao, Y.; Wargo, J. A.; Zheng, Z.; Xu, H.; Morgan, R. A.; Feldman, S. A.; Johnson, L. A.; Bennett, A. D.; Dunn, S. M.; Mahon, T. M.; Jakobsen, B. K.; Rosenberg, S. A. Single and dual amino acid substitutions in TCR CDRs can enhance antigen-specific T cell functions. *J. Immunol.* **2008**, *180*, 6116−6131.
(51) Robbins, P. F.; Kassim, S. H.; Tran, T. L.; Crystal, J. S.; Morgan, R. A.; Feldman, S. A.; Yang, J. C.; Dudley, M. E.; Wunderlich, J. R.; Sherry, R. M.; Kammula, U. S.; Hughes, M. S.; Restifo, N. P.; Raffeld, M.; Lee, C. C.; Li, Y. F.; El-Gamil, M.; Rosenberg, S. A. A pilot trial using lymphocytes genetically engineered with an NY-ESO-1-reactive T-cell receptor: long-term follow-up and correlates with response. *Clin. Cancer Res.* **2015**, *21*, 1019−1027.
(52) D'Angelo, S. P.; Melchiori, L.; Merchant, M. S.; Bernstein, D.; Glod, J.; Kaplan, R.; Grupp, S.; Tap, W. D.; Chagin, K.; Binder, G. K.; Basu, S.; Lowther, D. E.; Wang, R.; Bath, N.; Tipping, A.; Betts, G.; Ramachandran, I.; Navenot, J. M.; Zhang, H.; Wells, D. K.; Van Winkle, E.; Kari, G.; Trivedi, T.; Holdich, T.; Pandite, L.; Amado, R.; Mackall, C. L. Antitumor Activity Associated with Prolonged Persistence of Adoptively Transferred NY-ESO-1 (c259)T Cells in Synovial Sarcoma. *Cancer Discovery* **2018**, *8*, 944−957.
(53) Zuo, J.; Quinn, L. L.; Tamblyn, J.; Thomas, W. A.; Feederle, R.; Delecluse, H. J.; Hislop, A. D.; Rowe, M. The Epstein-Barr virus-encoded BILF1 protein modulates immune recognition of endoge-

https://doi.org/10.1021/acssynbio.1c00236
ACS Synth. Biol. 2022, 11, 1440−1453

nously processed antigen by targeting major histocompatibility complex class I molecules trafficking on both the exocytic and endocytic pathways. *J. Virol.* **2011**, *85*, 1604−1614.
(54) Itoh, Y.; Germain, R. N. Single cell analysis reveals regulated hierarchical T cell antigen receptor signaling thresholds and intraclonal heterogeneity for individual cytokine responses of CD4+ T cells. *J. Exp. Med.* **1997**, *186*, 757−766.
(55) Au-Yeung, B. B.; Smith, G. A.; Mueller, J. L.; Heyn, C. S.; Jaszczak, R. G.; Weiss, A.; Zikherman, J. IL-2 Modulates the TCR Signaling Threshold for CD8 but Not CD4 T Cell Proliferation on a Single-Cell Level. *J. Immunol.* **2017**, *198*, 2445−2456.
(56) Ashouri, J. F.; Weiss, A. Endogenous Nur77 Is a Specific Indicator of Antigen Receptor Signaling in Human T and B Cells. *J. Immunol.* **2017**, *198*, 657−668.
(57) Moran, A. E.; Holzapfel, K. L.; Xing, Y.; Cunningham, N. R.; Maltzman, J. S.; Punt, J.; Hogquist, K. A. T cell receptor signal strength in Treg and iNKT cell development demonstrated by a novel fluorescent reporter mouse. *J. Exp. Med.* **2011**, *208*, 1279−1289.
(58) Xi-zhi, J. G.; Dash, P.; Calverley, M.; Tomchuck, S.; Dallas, M. H.; Thomas, P. G. Rapid cloning, expression, and functional characterization of paired $\alpha\beta$ and $\gamma\delta$ T-cell receptor chains from single-cell analysis. *Mol. Ther.-Methods Clin. Dev.* **2016**, *3*, No. 15054.
(59) Smith, E. L.; Harrington, K.; Staehr, M.; Masakayan, R.; Jones, J.; Long, T. J.; Ng, K. Y.; Ghoddusi, M.; Purdon, T. J.; Wang, X.; Do, T.; Pham, M. T.; Brown, J. M.; De Larrea, C. F.; Olson, E.; Peguero, E.; Wang, P.; Liu, H.; Xu, Y.; Garrett-Thomson, S. C.; Almo, S. C.; Wendel, H. G.; Riviere, I.; Liu, C.; Sather, B.; Brentjens, R. J. GPRC5D is a target for the immunotherapy of multiple myeloma with rationally designed CAR T cells. *Sci. Transl. Med.* **2019**, *11*, No. eaau7746.
(60) Eyquem, J.; Mansilla-Soto, J.; Giavridis, T.; van der Stegen, S. J.; Hamieh, M.; Cunanan, K. M.; Odak, A.; Gonen, M.; Sadelain, M. Targeting a CAR to the TRAC locus with CRISPR/Cas9 enhances tumour rejection. *Nature* **2017**, *543*, 113−117.
(61) Roth, T. L.; Puig-Saus, C.; Yu, R.; Shifrut, E.; Carnevale, J.; Li, P. J.; Hiatt, J.; Saco, J.; Krystofinski, P.; Li, H.; Tobin, V.; Nguyen, D. N.; Lee, M. R.; Putnam, A. L.; Ferris, A. L.; Chen, J. W.; Schickel, J. N.; Pellerin, L.; Carmody, D.; Alkorta-Aranburu, G.; Del Gaudio, D.; Matsumoto, H.; Morell, M.; Mao, Y.; Cho, M.; Quadros, R. M.; Gurumurthy, C. B.; Smith, B.; Haugwitz, M.; Hughes, S. H.; Weissman, J. S.; Schumann, K.; Esensten, J. H.; May, A. P.; Ashworth, A.; Kupfer, G. M.; Greeley, S. A. W.; Bacchetta, R.; Meffre, E.; Roncarolo, M. G.; Romberg, N.; Herold, K. C.; Ribas, A.; Leonetti, M. D.; Marson, A. Reprogramming human T cell function and specificity with non-viral genome targeting. *Nature* **2018**, *559*, 405−409.
(62) Wang, J.; DeClercq, J. J.; Hayward, S. B.; Li, P. W.; Shivak, D. A.; Gregory, P. D.; Lee, G.; Holmes, M. C. Highly efficient homology-driven genome editing in human T cells by combining zinc-finger nuclease mRNA and AAV6 donor delivery. *Nucleic Acids Res.* **2016**, *44*, No. e30.
(63) Winoto, A.; Littman, D. R. Nuclear hormone receptors in T lymphocytes. *Cell* **2002**, *109*, S57−S66.
(64) Jennings, E.; Elliot, T. A. E.; Thawait, N.; Kanabar, S.; Yam-Puc, J. C.; Ono, M.; Toellner, K. M.; Wraith, D. C.; Anderson, G.; Bending, D.) Nr4a1 and Nr4a3 Reporter Mice Are Differentially Sensitive to T Cell Receptor Signal Strength and Duration. *Cell Rep.* **2020**, *33*, No. 108328.
(65) Webster, B.; Xiong, Y.; Hu, P.; Wu, D.; Alabanza, L.; Orentas, R. J.; Dropulic, B.; Schneider, D. Self-driving armored CAR-T cells overcome a suppressive milieu and eradicate CD19(+) Raji lymphoma in preclinical models. *Mol. Ther.* **2021**, 2691−2706.
(66) Kagoya, Y.; Tanaka, S.; Guo, T.; Anczurowski, M.; Wang, C. H.; Saso, K.; Butler, M. O.; Minden, M. D.; Hirano, N. A novel chimeric antigen receptor containing a JAK-STAT signaling domain mediates superior antitumor effects. *Nat. Med.* **2018**, *24*, 352−359.
(67) Jutz, S.; Leitner, J.; Schmetterer, K.; Doel-Perez, I.; Majdic, O.; Grabmeier-Pfistershammer, K.; Paster, W.; Huppa, J. B.; Steinberger, P. Assessment of costimulation and coinhibition in a triple parameter T cell reporter line: Simultaneous measurement of NF-kappaB, NFAT and AP-1. *J. Immunol. Methods* **2016**, *430*, 10−20.

https://doi.org/10.1021/acssynbio.1c00236
ACS Synth. Biol. 2022, 11, 1440−1453